Article

Origin of the S2 Benzylic Effect

Boris Galabov, Valia Nikolova, Jeremiah J. Wilke, Henry F. Schaefer III, and Wesley D. Allen

J. Am. Chem. Soc., **2008**, 130 (30), 9887-9896 • DOI: 10.1021/ja802246y • Publication Date (Web): 03 July 2008

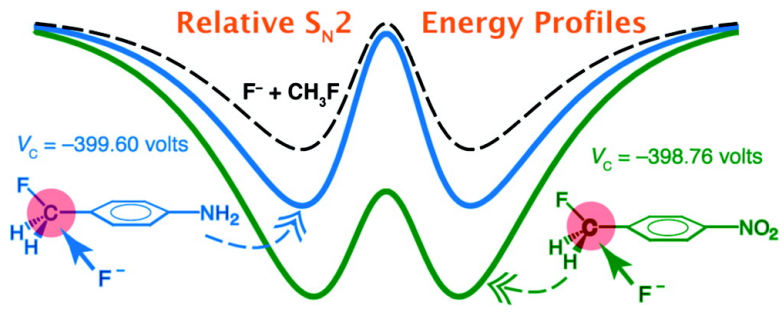

More About This Article

Additional resources and features associated with this article are available within the HTML version:

- Supporting Information
- Access to high resolution figures
- Links to articles and content related to this article
- Copyright permission to reproduce figures and/or text from this article

View the Full Text HTML

J|A|C|S
ARTICLES

Published on Web 07/03/2008

Origin of the S_N2 Benzylic Effect

Boris Galabov,[†] Valia Nikolova,[†] Jeremiah J. Wilke,[‡] Henry F. Schaefer III,[‡] and Wesley D. Allen*,[‡]

Department of Chemistry, University of Sofia, Sofia 1164, Bulgaria, and Center for Computational Chemistry and Department of Chemistry, University of Georgia, Athens, Georgia 30602

Received March 27, 2008; E-mail: wdallen@uga.edu

Abstract: The S_N2 identity exchange reactions of the fluoride ion with benzyl fluoride and 10 para-substituted derivatives ($RC_6H_4CH_2F$, R = CH_3, OH, OCH_3, NH_2, F, Cl, CCH, CN, COF, and NO_2) have been investigated by both rigorous ab initio methods and carefully calibrated density functional theory. Groundbreaking focal-point computations were executed for the $C_6H_5CH_2F + F^-$ and $C_6H_5CH_2Cl + Cl^-$ S_N2 reactions at the highest possible levels of electronic structure theory, employing complete basis set (CBS) extrapolations of aug-cc-pV*X*Z (*X* = 2−5) Hartree−Fock and MP2 energies, and including higher-order electron correlation via CCSD/aug-cc-pVQZ and CCSD(T)/aug-cc-pVTZ coupled cluster wave functions. Strong linear dependences are found between the computed electrostatic potential at the reaction-center carbon atom and the effective S_N2 activation energies within the series of para-substituted benzyl fluorides. An activation strain energy decomposition indicates that the S_N2 reactivity of these benzylic compounds is governed by the intrinsic electrostatic interaction between the reacting fragments. The delocalization of nucleophilic charge into the aromatic ring in the S_N2 transition states is quite limited and should not be considered the origin of benzylic acceleration of S_N2 reactions. Our rigorous focal-point computations validate the benzylic effect by establishing S_N2 barriers for (F^-, Cl^-) identity exchange in ($C_6H_5CH_2F$, $C_6H_5CH_2Cl$) that are lower than those of (CH_3F, CH_3Cl) by (3.8, 1.6) kcal mol^{-1}, in order.

Introduction

The mechanism of the S_N2 reaction is well established from myriad experimental kinetic and theoretical studies.[1–18] A full understanding of the chemistry of such processes requires a detailed knowledge of the structural factors pertinent to reactivity. Therefore, the effects of structural variations in both substrate and nucleophile have received considerable attention. Though many studies have focused on reactions of methyl or simple α-substituted methyl derivatives, more complex systems such as allyl halides and especially benzyl halides have also been subject to experimental and quantum chemical investigations.[19–25] The benzylic systems are intriguing because of the "benzylic effect", a marked increase in S_N2 reaction rates compared to analogous alkyl derivatives.[19,25–28] An appealing explanation of this effect in terms of classic bonding concepts

[†] University of Sofia.
[‡] University of Georgia.

(1) Shaik, S. S.; Schlegel, H. B.; Wolfe, S. *Theoretical Aspects of Physical Organic Chemistry: The S_N2 Mechanism*; Wiley & Sons: New York, 1992.
(2) Moylan, C. R.; Brauman, J. I. In *Advances in Classical Trajectory Methods*; JAI Press Inc.: London, 1994; Vol. 2, p 95.
(3) Brauman, J. I.; Olmstead, W. N.; Lieder, C. A. *J. Am. Chem. Soc.* **1974**, *96*, 4030–4031.
(4) Olmstead, W. N.; Brauman, J. I. *J. Am. Chem. Soc.* **1977**, *99*, 4219–4228.
(5) Asubiojo, O. I.; Brauman, J. I. *J. Am. Chem. Soc.* **1979**, *101*, 3715–3724.
(6) Pross, A.; Shaik, S. S. *New J. Chem.* **1989**, *13*, 427–433.
(7) DePuy, C. H.; Gronert, S.; Mullin, A.; Bierbaum, V. M. *J. Am. Chem. Soc.* **1990**, *112*, 8650–8655.
(8) Wladkowski, B. D.; Lim, K. F.; Allen, W. D.; Brauman, J. I. *J. Am. Chem. Soc.* **1992**, *114*, 9136–9153.
(9) Wolfe, S.; Mitchell, D. J. *J. Am. Chem. Soc.* **1981**, *103*, 7692–7694.
(10) Li, C.; Ross, P.; Szulejko, J. E.; McMahon, T. B. *J. Am. Chem. Soc.* **1996**, *118*, 9360–9367.
(11) Wilbur, J. L.; Brauman, J. I. *J. Am. Chem. Soc.* **1994**, *116*, 9216–9221.
(12) Takeuchi, K.; Takasuka, M.; Shiba, E.; Kinoshita, T.; Okazaki, T.; Abboud, J.-L. M.; Notario, R.; Castano, O. *J. Am. Chem. Soc.* **2000**, *122*, 7351–7357.
(13) Glukhovtsev, M. N.; Bach, R. D.; Pross, A.; Radom, L. *Chem. Phys. Lett.* **1996**, *260*, 558–564.
(14) Mo, Y. R.; Gao, J. L. *J. Comput. Chem.* **2000**, *21*, 1458–1469.
(15) Parthiban, S.; de Oliveira, G.; Martin, J. M. L. *J. Phys. Chem. A* **2001**, *105*, 895–904.
(16) Gonzales, J. M.; Cox, R. S.; Braun, S. T.; Allen, W. D.; Schaefer, H. F. *J. Phys. Chem. A* **2002**, *105*, 11327–11346.
(17) Gonzales, J. M.; Pak, C.; Cox, R. S.; Allen, W. D.; Schaefer, H. F.; Császár, A. G.; Tarcsay, G. *Chem.—Eur. J.* **2003**, *9*, 2173–2192.
(18) Gonzales, J. M.; Allen, W. D.; Schaefer, H. F. *J. Phys. Chem. A* **2005**, *109*, 10613–10628.
(19) Kost, D.; Aviram, K. *J. Am. Chem. Soc.* **1986**, *108*, 2006–2013.
(20) Wladkowski, B. D.; Wilbur, J. L.; Brauman, J. I. *J. Am. Chem. Soc.* **1994**, *116*, 2471–2480.
(21) Bordwell, F. G.; Hughes, D. L. *J. Org. Chem.* **1983**, *48*, 2206–2215.
(22) Bordwell, F. G.; Hughes, D. L. *J. Am. Chem. Soc.* **1984**, *106*, 2234–2240.
(23) Bordwell, F. G.; Hughes, D. L. *J. Org. Chem.* **1980**, *45*, 3314–3320.
(24) Lee, I.; Kim, B. S. *J. Comput. Chem.* **1995**, *16*, 1045–1054.
(25) Lee, I.; Kim, C. K.; Lee, B. S. *J. Phys. Org. Chem.* **1995**, *8*, 473–483.
(26) King, J. F.; Tsang, G. T. Y. *J. Chem. Soc., Chem. Commun.* **1979**, 1131–1132.
(27) Lynas, J. I.; Stirling, C. J. M. *J. Chem. Soc., Chem. Commun.* **1984**, 483–484.
(28) Amyes, T. L.; Jencks, W. P. *J. Am. Chem. Soc.* **1989**, *111*, 7900–7909.

is that the benzylic transition-state energy is lowered by delocalization of the nucleophilic electrons into the aromatic ring; however, for benzyl chloride systems, resonance stabilization of S_N2 transition states appears to be unimportant.[20] Understanding the influence on reactivity of substituents in the aromatic ring is difficult. Many experimental kinetic studies in solution have established "unusual" U-shaped Hammett plots,[29–33] indicating that both electron-withdrawing and electron-donating substituents enhance the reaction rate. The unusual features of S_N2 reactions of benzyl compounds have been explained in terms of differing mechanisms of substituent influence (electrostatic versus resonance effects), as well as possible crossovers from S_N2 to S_N1 mechanistic pathways.[34–47]

Because solvent effects in S_N2 processes can be very strong, gas-phase experiments have been used to expose the intrinsic effects of structural variations on the reactivity of benzylic systems.[41–45] Likewise, quantum mechanical computations on isolated systems have explored the essential influence of aromatic substituents in benzylic reactions.[11,24,25,46,47] In 1995, the Hartree−Fock (HF) and MP2 methods were applied to an allylic model system, $CH_2{=}CHCH_2X + X^-$, to interpret the S_N2 benzylic effect, implicating the stronger electron-accepting ability of the phenyl group in benzyl compounds.[25] In a comprehensive 1994 experimental study combined with AM1 semiempirical computations, Wladkowski et al.[20] investigated intrinsic structure−reactivity relationships for the gas-phase identity exchange reactions of substituted benzyl chlorides with chloride ion. The activation energies and prereaction complexation energies for benzyl chloride and five meta-substituted derivatives were measured, and computations were carried out for a larger series of derivatives. Both the experimental activation energies and the corresponding theoretical estimates correlated qualitatively with the Hammett σ constants of the substituents. Electron-withdrawing substituents enhanced the reactivity of benzyl chlorides, while electron-donating groups had the opposite effect. The stabilization of the intermediate ion−molecule complex and the S_N2 transition state was found to be similar for each substituent, suggesting that the reactivity of benzyl chlorides is influenced primarily by electrostatic rather than resonance effects.

Scheme 1. Series of S_N2 Reactions for Analysis of the Benzylic Effect[a]

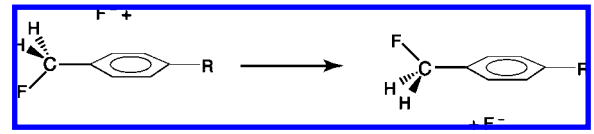

[a] R = H, CH_3, OH, OCH_3, NH_2, F, Cl, CN, NO_2, COF, and CCH.

The past decade has seen continuing research on structure−reactivity relationships for S_N2 reactions. The review of Brauman and co-workers[48] is particularly relevant. Kim et al.[49] used the PM3 semiempirical molecular-orbital method to analyze substituent effects in S_N2 reactions of benzyl chloride derivatives with phenoxides and thiophenoxides. Zhong and Brauman[50] examined the structure−reactivity relationships for the gas-phase identity exchange reactions of benzoyl chlorides with chloride ion, discovering that activation energies and complexation energies were *not* shifted equally by various substituents on the aromatic ring, unlike the benzyl chloride case. Kormos and Cramer[51] applied theoretical methods to the reactions of allyl chloride and its γ-methylated analogues with chloride anion. Computational studies also analyzed the steric retardation of the S_N2 reactions of some alkyl chlorides as well as α-cyanoalkyl derivatives.[52] Streitwieser et al.[53] used HF/6-31+G(d) computations to study substituent effects on S_N2 reactions of allyl halide derivatives with chloride and fluoride ions. An absence of conjugative stabilization of the transition states was found. The high reactivity of allyl halides was ascribed to electrostatic polarization of the double bond. Ochran and Uggerud[54] applied higher levels of theory to study the effects of structural variations and attacking nucleophile on the barrier heights of S_N2 reactions of allylic substrates. Finally, Ruff et al.[55,56] very recently executed B3LYP/6-31G(d) density functional computations on the nucleophilic substitution mechanisms of benzyl chlorides and benzyl bromides both in vacuo and in solution, finding fascinating variations in reactivity engendered by electron-withdrawing and electron-donating substituents.

In the present study, the benzylic effect is confirmed and quantified by a series of massive MP2 and coupled cluster computations to ascertain reliable S_N2 barriers for the $C_6H_5CH_2F + F^-$ and $C_6H_5CH_2Cl + Cl^-$ archetypes. Subsequently, B3LYP density functional theory is used to analyze the factors governing S_N2 fluoride identity exchange reactions within the series of para-substituted benzyl fluorides shown in Scheme 1. The distant

(29) Hudson, R. F.; Klopman, G. *J. Chem. Soc.* **1962**, 1062–1067.
(30) Fuchs, R.; Carlton, D. M. *J. Org. Chem.* **1962**, *27*, 1520–1523.
(31) Grimsrud, E. P.; Taylor, J. W. *J. Am. Chem. Soc.* **1970**, *92*, 739–741.
(32) Thorstenson, T.; Ellason, R.; Songstad, J. *Acta Chem. Scand., Ser. A* **1977**, *31*, 276–280.
(33) Young, P. R.; Jencks, W. P. *J. Am. Chem. Soc.* **1979**, *101*, 3288–3294.
(34) Johnson, C. D. *The Hammett Equation*; Cambridge University Press: New York, 1973.
(35) Ballistreri, F. P.; Maccarone, E.; Mamo, A. *J. Org. Chem.* **1976**, *41*, 3364–3367.
(36) Kaspi, J.; Rappoport, Z. *Tetrahedron Lett.* **1977**, *18*, 2035–2038.
(37) Aronovitch, H.; Pross, A. *Tetrahedron Lett.* **1977**, *18*, 2729–2732.
(38) Graczyk, D. G.; Taylor, J. W.; Turnquist, C. R. *J. Am. Chem. Soc.* **1978**, *100*, 7333–7339.
(39) Bordwell, F. G.; Hughes, D. L. *J. Org. Chem.* **1980**, *45*, 3320–3325.
(40) Pross, A.; Shaik, S. S. *J. Am. Chem. Soc.* **1981**, *103*, 3702–3709.
(41) Caldwell, G.; Magnera, T. F.; Kebarle, P. *J. Am. Chem. Soc.* **1984**, *106*, 959–966.
(42) DePuy, C. H.; Beedle, E. C.; Bierbaum, V. M. *J. Am. Chem. Soc.* **1982**, *104*, 6483–6488.
(43) DePuy, C. H.; Gronert, S.; Mullin, A.; Bierbaum, V. M. *J. Am. Chem. Soc.* **1990**, *112*, 8650–8655.
(44) Gronert, S.; DePuy, C. H.; Bierbaum, V. M. *J. Am. Chem. Soc.* **1991**, *113*, 4009–4010.
(45) Pellerite, M. J.; Brauman, J. I. *J. Am. Chem. Soc.* **1980**, *102*, 5993–5999.
(46) Davidson, R. B.; Williams, C. R. *J. Am. Chem. Soc.* **1978**, *100*, 73–79.
(47) Carrion, F.; Dewar, M. J. S. *J. Am. Chem. Soc.* **1984**, *106*, 3531–3539.
(48) Chabinyc, M. L.; Craig, S. L.; Regan, C. K.; Brauman, J. I. *Science* **1998**, *279*, 1882–1886.
(49) Kim, W. K.; Ryu, W. S.; Han, I. S.; Kim, C. K.; Lee, I. *J. Phys. Org. Chem.* **1998**, *11*, 115–124.
(50) Zhong, M. L.; Brauman, J. I. *J. Am. Chem. Soc.* **1999**, *121*, 2508–2515.
(51) Kormos, B. L.; Cramer, C. J. *J. Org. Chem.* **2003**, *68*, 6375–6386.
(52) Vayner, G.; Houk, K. N.; Jorgensen, W. L.; Brauman, J. I. *J. Am. Chem. Soc.* **2004**, *126*, 9054–9058.
(53) Streitwieser, A.; Jayastrae, E. G.; Leung, S. S.-H.; Choy, G. S.-C *J. Org. Chem.* **2005**, *70*, 8486–8491.
(54) Ochran, R. A.; Uggerud, E. *Int. J. Mass Spectrom.* **2007**, *265*, 169–175.
(55) Ruff, F.; Farkas, O.; Kucsman, A. *Eur. J. Org. Chem.* **2006**, 5570–5580.
(56) Ruff, F.; Farkas, O. *J. Phys. Org. Chem.* **2008**, *21*, 53–61.

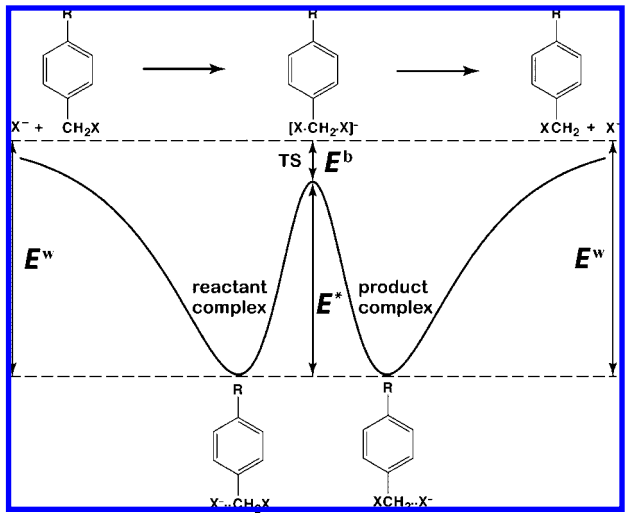

Figure 1. Energy profile of S_N2 identity exchange reactions of benzyl derivatives.

variations of structure with respect to the reaction center in these derivatives, as well as the absence of specific steric influences, is intended to reveal the intrinsic features of the S_N2 benzylic effect and thus contribute to the understanding of S_N2 reactivity in general.

Theoretical Methods

The geometric structures of the reactants, reactant ion−molecule complexes, transition states, product ion−molecule complexes, and products of the 11 S_N2 systems in Scheme 1 were fully optimized by use of the B3LYP hybrid density functional[57–59] combined with a standard DZP++ basis set. Cartesian coordinates and total energies for all optimized geometric structures are tabulated in Supporting Information. The DZP++ basis set consisted of the double-ζ sp contractions of Dunning[60–62] augmented with one set of polarization functions and a set of diffuse functions (s for hydrogen, s and p for heavy atoms). The diffuse functions were even tempered, following the suggestions of Lee and Schaefer.[63] The DZP++ basis set used in the present work is identical to the DZP+dif basis used in our previous studies on S_N2 systems and fully specified therein.[16–18]

High-level wave function methods were used to determine the energetics of the $C_6H_5CH_2F + F^-$ and $C_6H_5CH_2Cl + Cl^-$ identity exchange reactions within the established focal-point approach (FPA).[17,64–68] In the present application of this convergent, composite scheme, electron correlation was accounted for by second-order Møller−Plesset perturbation theory (MP2) and the coupled-cluster (CC) method including single and double excitations (CCSD) plus a perturbative treatment of connected triple excitations [CCSD(T)].[69–74] All correlation computations involved single-configuration restricted Hartree−Fock (RHF) reference wave functions. The cc-pV*X*Z and aug-cc-pV*X*Z [$X = 2$(D), 3(T), 4(Q), 5] families of correlation-consistent, atom-centered Gaussian basis sets[75–77] were employed, which give superior performance in systematically approaching the complete basis set (CBS) limit for correlated wave functions. Generally, the aug-cc-pV*X*Z sets were utilized to give added flexibility for diffuse electron clouds, but in the arduous coupled cluster computations it proved more practical and sufficient to use nonaugmented cc-pVXZ sets for the 10 atoms outside the immediate region of the S_N2 displacements.[78] In this paper, we designate the collective molecular basis sets according to the aug-cc-pV*X*Z set of functions providing the essential description of the reaction center. The largest, aug-cc-pV5Z basis sets utilized here contained 1703 and 1711 contracted functions for the $C_6H_5CH_2F/F^-$ and $C_6H_5CH_2Cl/Cl^-$ systems, respectively. In the focal-point analyses, series of RHF/aug-cc-pV*X*Z energies ($X = 3, 4, 5$) were extrapolated to the CBS limit by use of a three-parameter exponential function:[79]

$$E_X^{\mathrm{HF}} = E_{\mathrm{CBS}}^{\mathrm{HF}} + a\mathrm{e}^{-bX} \quad (1)$$

while MP2 electron correlation energies ($\varepsilon_X \equiv E_X^{\mathrm{MP2}} - E_X^{\mathrm{HF}}$, $X = 4,5$) were extrapolated with a widely utilized two-parameter polynomial formula:[80]

$$\varepsilon_X = \varepsilon_{\mathrm{CBS}} + bX^{-3} \quad (2)$$

Optimized MP2/DZP++ geometric structures were adopted for these extrapolations. Although the primary FPA computations froze the atomic core orbitals, auxiliary core correlation corrections (Δcore) were determined at the MP2 level with the cc-pCVTZ basis set.[81]

Rigorous ab initio wave function computations provide essential calibrations for the application of DFT methods to S_N2

(57) Becke, A. D. *J. Chem. Phys.* **1993**, *98*, 5648–5652.
(58) Becke, A. D. *J. Chem. Phys.* **1996**, *104*, 1040–1046.
(59) Lee, C. T.; Yang, W. T.; Parr, R. G. *Phys. Rev. B* **1988**, *37*, 785–789.
(60) Huzinaga, S. *J. Chem. Phys.* **1965**, *42*, 1293–1302.
(61) Dunning, T. H., Jr. *J. Chem. Phys.* **1970**, *53*, 2823–2833.
(62) Dunning, T. H., Jr. *Methods of Electronic Structure Theory*; Plenum Press: New York, 1977; Vol. 3, Chapt. 1.
(63) Lee, T. J.; Schaefer, H. F. *J. Chem. Phys.* **1985**, *83*, 1784–1794.
(64) East, A. L. L.; Allen, W. D. *J. Chem. Phys.* **1993**, *99*, 4638–4650.
(65) Schuurman, M. S.; Muir, S. R.; Allen, W. D.; Schaefer, H. F. *J. Chem. Phys.* **2004**, *120*, 11586–11599.
(66) Császár, A. G.; Tarczay, G.; Leininger, M. L.; Polyansky, O. L.; Tennyson, J.; Allen, W. D. In *Spectroscopy from Space*; Demaison, J., Sarka, K., Eds.; Kluwer: Dordrecht, The Netherlands, 2001; pp 317−339.
(67) Allen, W. D.; East, A. L. L.; Császár, A. G. In *Structures and Conformations of Non-Rigid Molecules*; Laane, J., Dakkouri, M., van der Veken, B., Oberhammer, H., Eds.; Kluwer: Dordrecht, The Netherlands, 1993; pp 343−373.
(68) Császár, A. G.; Allen, W. D.; Schaefer, H. F. *J. Chem. Phys.* **1998**, *108*, 9751–9764.
(69) Hehre, W. J.; Radom, L.; Schleyer, P. v. R. ; Pople, J. A. *Ab Initio Molecular Orbital Theory*; Wiley: New York, 1986.
(70) Čížek, J. *J. Chem. Phys.* **1966**, *45*, 4256–4266.
(71) Purvis, G. D.; Bartlett, R. J. *J. Chem. Phys.* **1982**, *76*, 1910–1918.
(72) Scuseria, G. E.; Janssen, C. L.; Schaefer, H. F. *J. Chem. Phys.* **1988**, *89*, 7382–7387.
(73) Crawford, T. D.; Schaefer, H. F. *Rev. Comput. Chem.* **2000**, *14*, 33–136.
(74) Raghavachari, K.; Trucks, G. W.; Pople, J. A.; Head-Gordon, M. *Chem. Phys. Lett.* **1989**, *157*, 479–483.
(75) (a) Dunning, T. H. Jr. *J. Chem. Phys.* **1989**, *90*, 1007–1023. (b) Wilson, A. K.; van Mourik, T.; Dunning, T. H., Jr. *J. Mol. Struct. (THEOCHEM)* **1996**, *388*, 339–349.
(76) Kendall, R. A.; Dunning, T. H., Jr.; Harrison, R. J. *J. Chem. Phys.* **1992**, *96*, 6796–6806.
(77) Woon, D. E.; Dunning, T. H., Jr. *J. Chem. Phys.* **1993**, *98*, 1358−1371; **1994**, *100*, 2975−2988.
(78) For the $C_6H_5CH_2F + F^-$ and $C_6H_5CH_2Cl + Cl^-$ reactions, paring the diffuse functions on the 10 peripheral atoms from the aug-cc-pVQZ basis set cuts the number of functions by 205 but alters the respective MP2 net barriers (E^b) by only +0.37 and +0.25 kcal mol^{-1}. The approximation used in this study should be substantially more accurate than these variations, because diffuse functions were pared only to compute CCSD/aug-cc-pVQZ and CCSD(T)/aug-cc-pVTZ *corrections* to the MP2 barriers. With the aug-cc-pVDZ basis set, this approximation changes the CCSD(T)−MP2 correction for the $C_6H_5CH_2F + F^-$ and $C_6H_5CH_2Cl + Cl^-$ barriers by only 0.04 and 0.11 kcal mol^{-1}, respectively.
(79) Feller, D. *J. Chem. Phys.* **1992**, *96*, 6104−6114; **1993**, *98*, 7059−7071.
(80) Helgaker, T.; Klopper, W.; Koch, H.; Noga, J. *J. Chem. Phys.* **1997**, *106*, 9639–9646.
(81) Woon, D. E.; Dunning, T. H., Jr. *J. Chem. Phys.* **1995**, *103*, 4572–4585.

reactions.[16–18,82,83] In particular, we have previously compared the energetics of a number of $CH_3X + Y^-$ reactions obtained at the B3LYP/DZP++ level of theory[16,18] with highly accurate focal-point extrapolations[17,18] that employed basis sets as large as aug-cc-pV5Z, electron correlation treatments as extensive as CCSD(T), and auxiliary corrections for core correlation and relativistic effects. A plot of B3LYP/DZP++ versus FPA net activation barriers for these S_N2 reactions is provided in Figure S1 of Supporting Information, where a nearly perfect linear dependence is exhibited with a correlation coefficient $r = 0.996$. Our extensive calibrations, discussed in more detail below, give confidence that the B3LYP net activation barriers computed in the present study are quite accurate and realistic for the reactions in Scheme 1. The B3LYP *trends* in reaction energetics under structural variations should be especially reliable for drawing conclusions about the origin of the S_N2 benzylic effect.

For interpretive purposes, B3LYP/DZP++ computations were executed to probe the molecular electrostatic potential experienced by the carbon atom at the S_N2 reaction center. The electrostatic potential at a particular nucleus (Y) positioned at $\mathbf{R}_Y$ is defined by eq 3 (in atomic units), where the singular term $\mathbf{R}_A = \mathbf{R}_Y$ has been excluded:[84,85]

$$V_Y \equiv V(\mathbf{R}_Y) = \sum_{A(\neq Y)} \frac{Z_A}{|\mathbf{R}_Y - \mathbf{R}_A|} - \int \frac{\rho(\mathbf{r}')}{|\mathbf{R}_Y - \mathbf{r}'|}\, d\mathbf{r}' \qquad (3)$$

In this equation Z_A is the charge on nucleus A, positioned at $\mathbf{R}_A$, while $\rho(\mathbf{r})$ is the electron density of the molecule. In addition, natural bond orbital (NBO) charges on the various atoms were derived from natural population analyses.[86,87]

In this study, the massive MP2/aug-cc-pV*X*Z computations were performed with MPQC;[88] the high-level coupled cluster results were obtained with the MOLPRO package;[89] and all DFT work was carried out with Gaussian 94.[90]

Results and Discussion

As depicted in Figure 1, there are three main quantities characterizing the energy profile of the double-well potential energy surface of gas-phase S_N2 reactions: (1) the complexation energy (E^w) of the pre- and postreaction ion−molecule complexes; (2) the central activation barrier (E^*), which is the height of the S_N2 transition state (TS) above the prereaction complex; and (3) the net activation barrier (E^b), defined as the energy difference between the transition state and the separated reactants. The most relevant parameter for comparing reactivities is the net activation barrier, E^b, which is also the quantity usually derived from experimental kinetic studies.[3–11]

The Benzylic Effect and Its Source. Before analyzing changes in reactivity upon structural variation within our series of benzyl fluorides, it is important to rigorously substantiate and quantify the S_N2 benzylic effect. The focal-point analyses to determine the net barriers (E^b) for the paradigmatic $C_6H_5CH_2F + F^-$ and $C_6H_5CH_2Cl + Cl^-$ identity exchange reactions are summarized in Table 1. The two-dimensional grid shows the convergence of E^b values toward both the atomic orbital basis (vertical) and the electron correlation (horizontal) limits. For both reactions, the aug-cc-pVQZ basis is necessary to come within 0.6 kcal mol^{-1} of the apparent CBS limits for all levels of theory. The signs and magnitudes of the correlation increments (δ) follow the statistical trends documented in our earlier high-level computations[17,18] for $CH_3X + Y^-$ (X = F, Cl, CN, OH, SH, NH_2, PH_2; Y = X or F) S_N2 reactions. In particular, the successive application of [MP2, CCSD, CCSD(T)] theory changes the net barriers in such S_N2 systems in a remarkably systematic manner by about (−10, +2, −3) kcal mol^{-1}. With inclusion of core correlation and zero-point vibrational energy (ZPVE), the final E^b values for the benzyl fluoride and benzyl chloride reactions are −4.6 and +0.2 kcal mol^{-1}, respectively. The accuracy of these predictions should be much better than 1 kcal mol^{-1} and is limited to any appreciable extent only by the effects of high-order electron correlation past the perturbative triples level of coupled cluster theory.

Table 1. Focal-Point Computations of the Net Activation Barrier for the S_N2 Identity Exchange Reactions of Benzyl Fluoride and Benzyl Chloride[a]

basis	ΔE_e[RHF]	δ[MP2]	δ[CCSD]	δ[CCSD(T)]	ΔE_e[CCSD(T)]
		$C_6H_5CH_2F + F^-$			
aug-cc-pVDZ	+5.87	−12.49	+2.23	−3.37	−7.77
aug-cc-pVTZ	+8.18	−12.29	+2.61	−3.61	−5.11
aug-cc-pVQZ	+8.33	−12.12	+2.79	[−3.61]	[−4.61]
aug-cc-pV5Z	+8.42	−11.93	[+2.79]	[−3.61]	[−4.33]
CBS limit	[+8.49]	[−11.73]	[+2.79]	[−3.61]	[−4.06]
final $E^b = \Delta E_e$[CCSD(T)/CBS] + Δcore[MP2/cc-pCVTZ] + ΔZPVE[MP2/DZP++] = −4.06 + 0.17 − 0.74 = **−4.63** kcal mol^{-1}					
		$C_6H_5CH_2Cl + Cl^-$			
aug-cc-pVDZ	+8.94	−9.97	+2.23	−3.07	−1.87
aug-cc-pVTZ	+10.41	−9.96	+2.91	−3.46	−0.10
aug-cc-pVQZ	+10.91	−9.87	+3.11	[−3.46]	[+0.69]
aug-cc-pV5Z	+11.18	−9.93	[+3.11]	[−3.46]	[+0.91]
CBS limit	[+11.32]	[−9.98]	[+3.11]	[−3.46]	[+0.99]
final $E^b = \Delta E_e$[CCSD(T)/CBS] + Δcore[MP2/cc-pCVTZ] + ΔZPVE[B3LYP/DZP++] = +0.99 − 0.07 − 0.68 = **+0.24** kcal mol^{-1}					

[a] Net activation barrier values (E^b) are given in kilocalories per mole. δ denotes computed increments in the vibrationless barrier, ΔE_e, with respect to the preceding level of theory. Brackets signify increments obtained from basis set extrapolations or additivity approximations.

The key energetic quantities (E^w, E^*, and E^b) for S_N2 identity exchange in benzyl fluoride and benzyl chloride are compared with analogous data for CH_3F and CH_3Cl in Table 2. The focal-point E^b computations for the chloride reactions are in excellent accord with the activation energies derived from Fourier transform ion cyclotron resonance ($C_6H_5CH_2Cl + Cl^-$, +0.2 kcal mol^{-1})[20] and Flowing Afterglow-SIFT-Drift ($CH_3Cl + Cl^-$, 1 ± 1 kcal mol^{-1})[91] rate measurements. The focal-point analysis definitively confirms the intrinsic benzylic effect, showing that substitution of an aromatic ring at the central carbon lowers the S_N2 net barriers of the methyl fluoride and methyl chloride reactions by 3.8 and 1.6 kcal mol^{-1}, respectively. Such changes in nearly thermoneutral activation barriers can indeed dramatically accelerate chemical reactions.

As detailed in Supporting Information (Table S1), the E^w quantities for the $C_6H_5CH_2F/F^-$ and $C_6H_5CH_2Cl/Cl^-$ complexes

(82) Stewart, M.; Solá, M.; Bickelhaupt, F. M. *J. Comput. Chem.* **2007**, *28*, 1551–1560.
(83) Bento, A. P.; Solá, M.; Bickelhaupt, F. M. *J. Comput. Chem.* **2005**, *26*, 1497–1504.
(84) Politzer, P. In *Chemical Applications of Atomic and Molecular Electrostatic Potentials*; Politzer, P., Truhlar, D. G., Eds.; Plenum Press: New York, 1981; pp 7−28.
(85) Wilson, E. B., Jr. *J. Chem. Phys.* **1962**, *36*, 2232–2233.
(86) Reed, A. E.; Weinstock, R. B.; Weinhold, F. *J. Chem. Phys.* **1985**, *83*, 735–746.
(87) Reed, A. E.; Curtiss, L. A.; Weinhold, F. *Chem. Rev.* **1988**, *88*, 899–926.
(88) Janssen, C. L.; Nielsen, I. B.; Leininger, M. L.; Valeev, E. F.; Seidl, E. T. *The Massively Parallel Quantum Chemistry Program (MPQC)*; Sandia National Laboratories, Livermore, CA, 2004.
(89) *MOLPRO*, version 2006.1; a package of ab initio programs written by Werner, H.-J., et al. For the latest version, see http://www.molpro.net.
(90) Frisch, M. J., et al. *Gaussian 94*, Revision C.3; Gaussian, Inc.: Pittsburgh, PA, 1995.
(91) Barlow, S. E.; Van Doren, J. M.; Bierbaum, V. M. *J. Am. Chem. Soc.* **1988**, *110*, 7240–7242.

Table 2. Comparison of Complexation Energies, Central Activation Barriers, and Net Activation Barriers for the S_N2 Identity Exchange Reactions of Methyl versus Benzyl Fluoride and Methyl versus Benzyl Chloride[a]

method	E^w (kcal mol^{-1})	E^* (kcal mol^{-1})	E^b (kcal mol^{-1})
	$CH_3F + F^-$		
B3LYP/DZP++[b]	−12.87	10.45	−2.42
FPA[b]	−13.73	12.93	−0.81
	$C_6H_5CH_2F + F^-$		
B3LYP/DZP++	−22.01	16.90	−5.11
FPA	−23.41	18.78	−4.63
	$CH_3Cl + Cl^-$		
B3LYP/DZP++[b]	−9.71	8.38	−1.31
FPA[b]	−11.03	12.88	+1.85
expt			+1 ± 1[c]
	$C_6H_5CH_2Cl + Cl^-$		
B3LYP/DZP++	−12.13	10.02	−2.11
FPA	−14.78	15.02	+0.24
expt			+0.2[d]

[a] All quantities include zero-point vibrational energy (ZPVE). [b] Reference 18. [c] Reference 91. [d] Reference 20.

were also determined by focal-point analyses. The $C_6H_5CH_2F/F^-$ complex is bound by 23.4 kcal mol^{-1}, a prodigious interaction energy almost 10 kcal mol^{-1} greater than in the CH_3F/F^- adduct. The benzylic change in E^w is much less in the chloride case but still very substantial (−3.8 kcal mol^{-1}). The increased binding energies of the benzyl versus methyl complexes are largely attributable to an additional stabilizing interaction of the halide ions with the closest hydrogen on the aromatic ring. In particular, the energy of the $C_6H_5CH_2F/F^-$ system is lowered by 8.4 kcal mol^{-1} (B3LYP/DZP++ level) when the fluoride ion migrates from a backside stationary point along the axis of S_N2 attack to a minimum positioned intermediate between a methylene and an aromatic hydrogen. Essentially, the halide ions in the benzylic complexes exhibit bifurcated hydrogen bonding distinct from the ion−molecule interactions in the methyl adducts, demanding caution in comparing respective E^w values.

The B3LYP/DZP++ method has a well-documented propensity[16–18] to systematically underestimate both S_N2 central barriers (E^*) and ion−molecule complexation energies (E^w), as seen in Table 2. The E^w effect mitigates E^* errors in determining net S_N2 barriers, but not enough in the CH_3F, CH_3Cl, and $C_6H_5CH_2Cl$ cases to avert E^b values that are too low by 1.6, 3.2, and 2.4 kcal mol^{-1}, respectively, vis-à-vis the focal-point benchmarks. However, for the $C_6H_5CH_2F + F^-$ system, more advantageous cancelation of errors leads to a B3LYP/DZP++ net barrier that is only 0.5 kcal mol^{-1} below our best focal-point prediction. For this reason, corrections to the B3LYP/DZP++ net barriers are not necessary for the series of reactions in Scheme 1, especially because we are concerned here with relative trends in the data.

Different hypotheses have been put forward to explain the greater S_N2 reactivity of benzylic compounds, as discussed above. Here we examine computed NBO atomic charges for the $C_6H_5CH_2F$, CH_3F, $C_6H_5CH_2Cl$, and CH_3Cl reactions to elucidate the benzylic effect, as presented in Figures 2 and 3. Although the NBO scheme is a superior tool for population analyses,[86,87] a caveat is that such atomic charges are model-dependent and not direct physical observables.

For the benzyl fluoride reaction, summing up the charge variations for the atoms of the aromatic system (carbons and hydrogens) yields a striking conclusion. Of the −1e charge that enters the system upon fluoride attack, only −0.07e is transferred to the aromatic ring in the S_N2 transition state. Moreover, the fluorine atoms in the benzylic transition state both carry charges of −0.69e, not much less than the corresponding charges of −0.72e in the methyl fluoride transition state. In brief, 93% of the excess negative charge coming from the fluoride anion stays effectively within the -CH_2F_2 moiety. The benzyl chloride analysis yields the same picture. Only −0.03e of the charge brought by chloride attack migrates to the aromatic ring in the transition state, and the chlorine atoms in the benzyl chloride TS actually carry slightly more negative charge than in the methyl chloride case. It is thus difficult to ascribe the energetic lowering of the transition state in the benzylic systems to the delocalization of the excess negative charge into the aromatic ring.

A compelling indication that nucleophilic attack on the benzyl halides does not significantly alter the electronic structure of the aromatic ring is the lack of variation in the carbon−carbon bond distances (r_{CC}). In the $C_6H_5CH_2F + F^-$ system, the range of r_{CC} values in the ring is merely 0.004 Å in *both* the reactant and transition state, and the individual distances change less than 0.002 Å in reaching the S_N2 col. In the $C_6H_5CH_2Cl$ reactant the span of ring distances is 0.006 Å, as compared to 0.011 Å in the transition state for Cl^- exchange, while r_{CC}(TS) never departs from r_{CC}(reactant) by more than 0.003 Å.

A more plausible explanation for the benzylic effect is suggested by the electrostatic potentials (V_C) and NBO charges at the reaction-center carbons. As shown in Figures 2 and 3, the NBO charge on the central carbon atom of benzyl fluoride and benzyl chloride is 0.16e and 0.20e more positive, respectively, than in the methyl analogues. Moreover, these differences are not altered more than 0.01e if the transition state structures are compared rather than the reactants. A more rigorous measure is that V_C(benzyl) is always greater than V_C(methyl) at the stationary points along the S_N2 reaction paths in both the fluoride and chloride systems.

Specific and forceful evidence that reactant electrostatics is key to the benzylic effect is found by comparing V_C potentials in the benzyl versus methyl ion−molecule complexes formed immediately prior to surmounting the central S_N2 barriers. These data are given in Figures 2 and 3. For the benzylic reactions the proper complexes for the comparison are obtained by enforcing C_s symmetry in the geometry optimizations to ensure that the attacking halide ions reside along the back side of the bond being broken by the S_N2 displacement; otherwise, the optimizations yield the distorted structures described above with bifurcated hydrogen bonding to the aromatic ring that do not correspond to the C_{3v} symmetry $X^-\cdot CH_3X$ adducts. For the prereaction complexes of the fluoride systems, V_C(benzyl) is 0.56 V greater than V_C(methyl), and this difference increases to 0.78 V in the S_N2 transition state. In the chloride case, V_C(benzyl) − V_C(methyl) = +0.56 V and +0.52 V for the complexes and transition states, respectively. These V_C data bolster the argument that the electrostatic attraction between the attacking halide anion and the reaction center is considerably stronger for the benzylic systems, resulting in lower S_N2 reaction barriers. More support for an electrostatic interpretation of the benzylic effect is provided by our analysis in the next section of substituent trends in S_N2 energetics.

Aromatic Substituent Effects. To investigate the consequences of chemical structure variations on S_N2 reactivity in benzylic systems, we selected a representative series of derivatives (Scheme 1) containing both electron-donating and

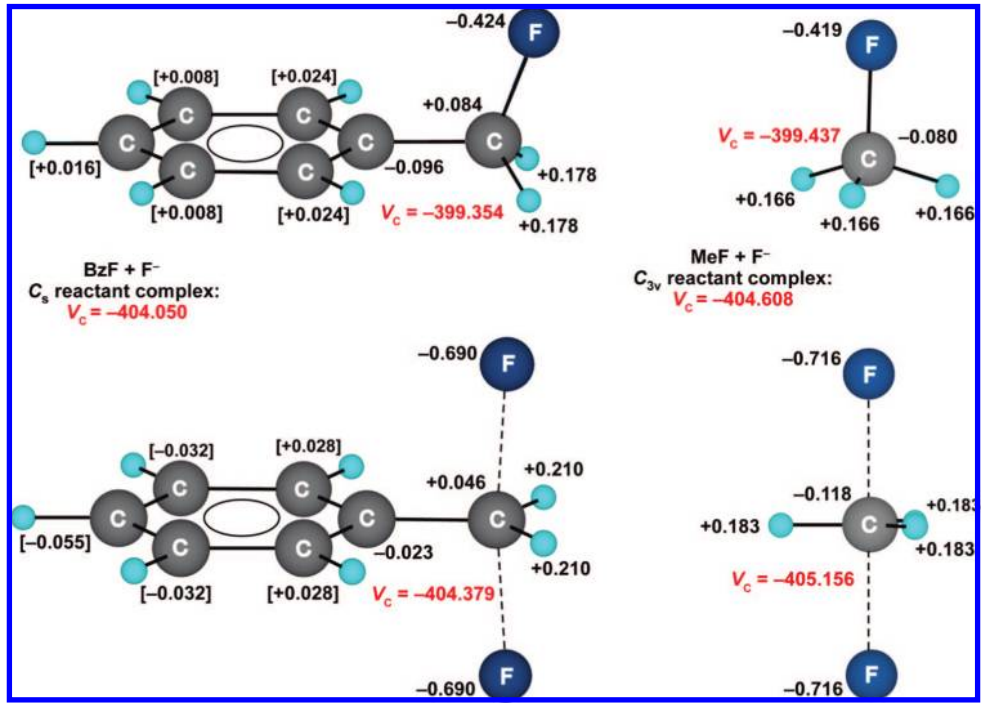

Figure 2. NBO atomic charges and electrostatic potential on the central carbon (V_C, in volts) for benzyl fluoride (BzF), methyl fluoride (MeF), their reactant ion−molecule complexes, and respective transition states for S_N2 identity exchange (B3LYP/DZP++ method). For ease of interpretation, the values shown in brackets around the aromatic ring are sums of NBO charges on the carbon atoms and the attached hydrogens.

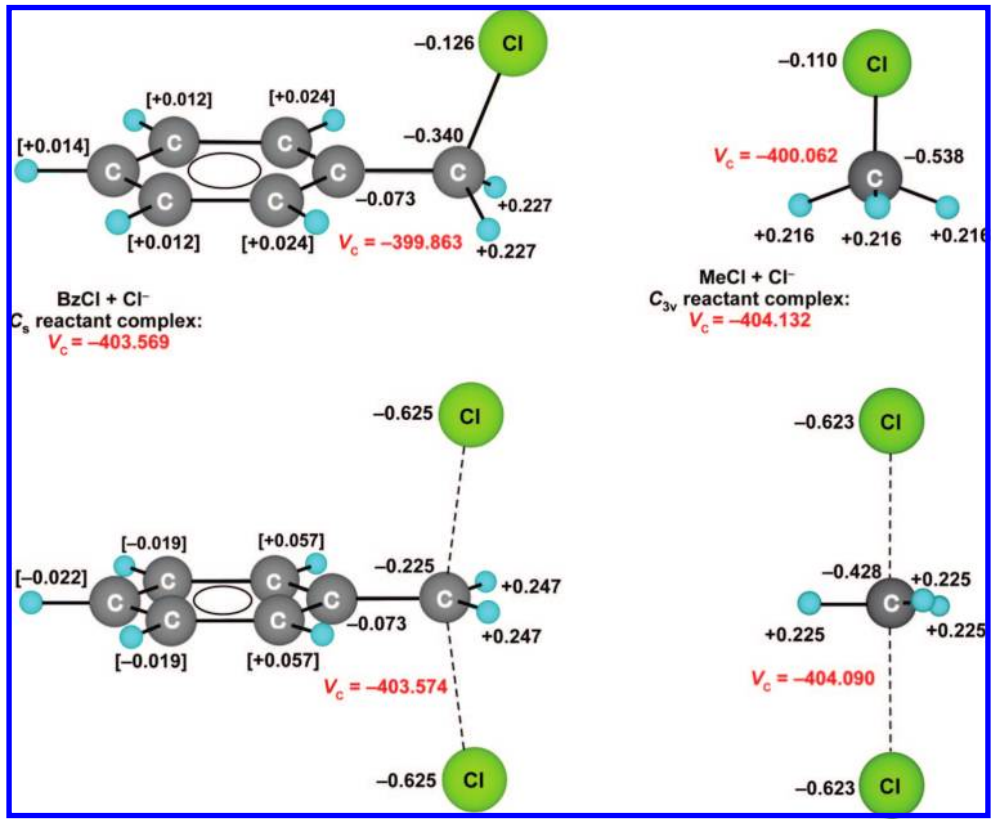

Figure 3. NBO atomic charges and electrostatic potential on the central carbon (V_C, in volts) for benzyl chloride (BzCl), methyl chloride (MeCl), their reactant ion−molecule complexes, and respective transition states for S_N2 identity exchange (B3LYP/DZP++ method). For ease of interpretation, the values shown in brackets around the aromatic ring are sums of NBO charges on the carbon atoms and the attached hydrogens.

electron-withdrawing substituents. Para-substitution was chosen in all of these derivatives to eliminate proximity effects on the reaction center. The B3LYP/DZP++ complexation energies (E^w), central activation barriers (E^*), and net activation barriers (E^b) for fluoride identity exchange are given in Table 3. In view of the literature findings of unusual

Table 3. B3LYP/DZP++ Complexation Energies, Central Activation Barriers, and Net Activation Barriers for S_N2 Reactions of Benzyl Fluoride Derivatives with Fluoride Ion[a]

substituent	E^w (kcal mol^{-1})	E^* (kcal mol^{-1})	E^b (kcal mol^{-1})	σ_p[b]
-H	−22.01	16.89	−5.11	0.0
p-CH_3	−21.09	16.93	−4.15	−0.17
p-OH	−22.68	18.22	−4.46	−0.37
p-OCH_3	−21.54	17.91	−3.63	−0.27
p-NH_2	−19.50	17.63	−1.87	−0.66
p-F	−25.42	17.54	−7.87	0.06
p-Cl	−26.71	17.28	−9.43	0.23
p-CN	−24.16	8.50	−15.66	0.66
p-NO_2	−28.82	10.78	−18.04	0.78
p-COF	−25.34	9.14	−16.20	0.70
p-CCH	−25.75	16.49	−9.26	0.23

[a] All quantities include zero-point vibrational energies (ZPVE). [b] Reference 92.

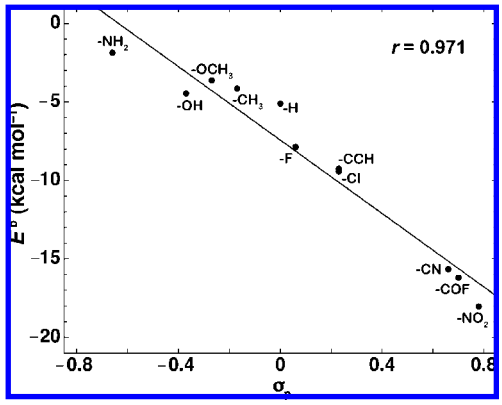

Figure 4. Relationship between net S_N2 activation barrier (E^b) and substituent Hammett σ constants for the reactions of Scheme 1. Data for linear fit: *y*-intercept = −7.43(44); slope = −11.69(96); linear regression coefficient (r) = 0.971.

Hammett plots for S_N2 reactions of benzylic systems, the σ constants of the substituents are also given in the table. It should be noted that these σ constants are determined from solution chemical equilibrium studies.[92]

For every benzylic compound in Table 3, the net activation barrier (E^b) is negative, which means that the S_N2 transition state lies below the energy of the reactants in the gas phase. Remarkably, the range of E^b variations is over 16 kcal mol^{-1}, demonstrating the effectiveness of the aromatic ring in transmitting electronic distortions engendered by the para substituents. Figure 4 plots the net activation barriers versus the Hammett σ constants of the derivatives. Though the correlation between the two quantities is not precise (linear correlation coefficient r = 0.971), the overall trend is not unusual. Electron-withdrawing substituents (-F, -Cl, -CN, -NO_2, -COF, and -CCH) lower the barrier considerably and enhance the S_N2 reaction rate, while electron-donating substituents (-CH_3, -OH, -OCH_3, and -NH_2) raise the barrier and reduce the S_N2 reaction rate. However, the effect of electron-donating substituents is much less pronounced than expected from the values of the σ constants. It is evident that S_N2 reactions of benzylic derivatives do not quite follow the usual reactivity trends for organic systems.[93,94]

Solvent influences on the experimental σ constants[92] obscure their intrinsic reactivity measures. Therefore, the search for alternative molecular properties for embodying concise, intrinsic structure−reactivity relationships is warranted. Motivated by the strong role identified above of electrostatics in the benzylic effect, we further investigated the electrostatic potential (V_C) at the reaction-center carbon atom as an indicator of intrinsic S_N2 reactivity. Previous studies on two solvolytic reactions[95,96] as well as hydrogen bonding[97–100] have revealed that the electrostatic potential at the atoms of reaction centers can provide an excellent measure of reactivities.

Table 4. B3LYP/DZP++ Net Activation Barriers and Electrostatic Potentials at the Reaction-Center Carbon Atom of Reactants and Transition States for the S_N2 Identity Exchange Reactions of Benzyl Fluorides

substituent	E^b (kcal mol^{-1})	V_C(reactant) + 398 (V)	V_C(TS) + 398 (V)
-H	−5.11	−1.354	−6.379
p-CH_3	−4.15	−1.448	−6.423
p-OH	−4.46	−1.414	−6.383
p-OCH_3	−3.63	−1.484	−6.412
p-NH_2	−1.87	−1.596	−6.489
p-F	−7.87	−1.186	−6.229
p-Cl	−9.43	−1.140	−6.123
p-CN	−15.66	−0.849	−5.806
p-NO_2	−18.04	−0.759	−5.646
p-COF	−16.20	−0.852	−5.764
p-CCH	−9.26	−1.210	−6.107

In Table 4, S_N2 net activation barriers are compiled alongside V_C values in the reactant and transition state for our series of benzylic derivatives. A striking linear dependence, with correlation coefficient r = 0.994, exists between V_C(reactant) and E^b, as illustrated in the top panel of Figure 5. Thus, the reactivity of the benzyl fluorides toward S_N2 identity exchange with fluoride ion is predicted very well by the pre-existing V_C values in the reactants. The bottom panel of Figure 5 reveals an even better linear correlation between the transition-state electrostatic potential [V_C(TS)] and the net barriers E^b. In essence, a strong structure−reactivity relationship is established in two steps: the net S_N2 barrier is largely determined by electrostatic effects in the transition state that are embedded in V_C(TS), and in turn the V_C(TS) values are closely correlated with the corresponding V_C potentials in the reactants.

Finally, V_C potentials cannot be replaced simplistically by NBO charges as a satisfactory index of intrinsic S_N2 reactivity in these systems. For the para-substituted benzyl fluoride reactants, the NBO charge at the reaction-center carbon (q_C) lies in too narrow a range (+0.0805e to +0.0842e) to contain much information about the eventual barrier, and the plot of E^b versus q_C is scattered. Apparently, q_C in isolation is not a sufficiently sensitive measure of the regional electrostatics that influence the S_N2 reactions. Another gauge is the degree to which E^b can be associated with the nucleophilic charge transferred to the aromatic ring in the S_N2 transition states (q_{ct}). Over the entire series, the NBO method computes q_{ct} from −0.065e to −0.105e (Figure S2 in Supporting Information),

(92) (a) Hammett, L. P. *Physical Organic Chemistry*; McGraw-Hill: New York, 1940. (b) McDaniel, D. H.;; Brown, H. C. *J. Org. Chem.* **1958**, *23*, 420–427.
(93) Jaffe, H. H. *Chem. Rev.* **1953**, *53*, 191–261.
(94) Hansch, C.; Leo, A.; Taft, R. W. *Chem. Rev.* **1991**, *91*, 165–195.
(95) Galabov, B.; Cheshmedzhieva, D.; Ilieva, S.; Hadjieva, B. *J. Phys. Chem. A* **2004**, *108*, 11457–11462.
(96) Galabov, B.; Atanassov, Y.; Ilieva, S.; Schaefer, H. F. *J. Phys. Chem. A* **2005**, *109*, 11470–11474.
(97) Bobadova-Parvanova, P.; Galabov, B. *J. Phys. Chem. A* **1998**, *102*, 1815–1819.
(98) Galabov, B.; Bobadova-Parvanova, P. *J. Phys. Chem. A* **1999**, *103*, 6793–6799.
(99) Dimitrova, V.; Ilieva, S.; Galabov, B. *J. Phys. Chem. A* **2002**, *106*, 11801–11805.
(100) Galabov, B.; Bobadova-Parvanova, P.; Ilieva, S.; Dimitrova, V. *J. Mol. Struct. (THEOCHEM)* **2003**, *630*, 101–112.

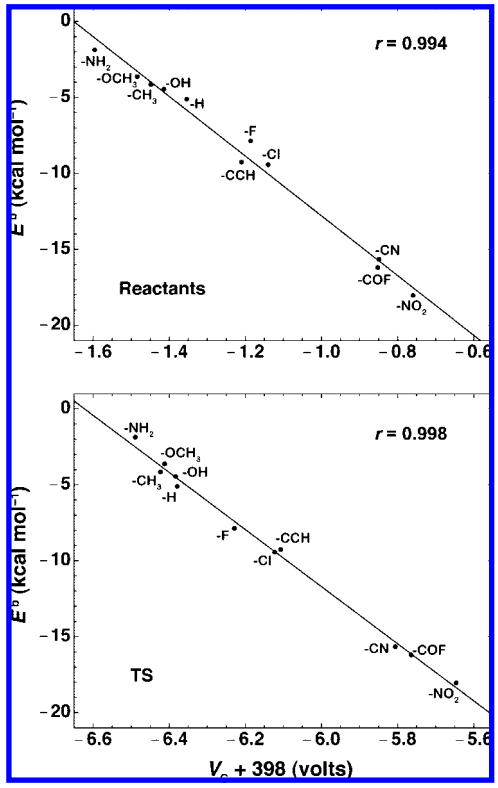

Figure 5. Relationship between the net S_N2 activation barrier (E^b) and the reaction-center electrostatic potential (V_C) for the substituted benzyl fluorides of Scheme 1. V_C is plotted for the central carbon atom in the isolated reactant (top panel) and the S_N2 transition state (TS) (bottom panel). Data for linear fits [top, bottom]: y-intercept = [−32.45(94), −124.5(27)]; slope = [−19.66(76), −18.80(44)]; linear regression coefficient (r) = [0.994, 0.998].

values generally more consistent with an induction mechanism rather than resonance delocalization. Within this window, the (E^b, q_{ct}) data display a modest correlation ($r = 0.956$) but there are some serious disparities, such as (E^b, q_{ct}) = (−9.26, −0.0855) for p-CCH but (−9.43, −0.0758) for p-Cl. The (E^b, q_{ct}) relationship can be explained as a secondary correlation: those aromatic substituents that best raise the electrostatic potential at the reaction center, the primary influence on E^b, are the same ones that inductively pull a little extra charge into the ring. Of course, the relationship between V_C and q_{ct} is intricate, a complicated outcome of the quantum mechanical behavior of the many-electron system. Nonetheless, it is clear that NBO charges are not nearly as good as the model-independent parameter V_C in measuring the principal interactions governing the benzylic S_N2 reactions.

Activation Strain Analysis. The strong correlation in our benzylic systems between the electrostatic potential at the reaction-center carbon and the net S_N2 activation barrier can be explained nicely in terms of the activation strain (AS) model of Bickelhaupt and co-workers.[101–106] The AS model is a fragment approach in which the height of reaction barriers is decomposed into two terms: (a) the energy (ΔE_{strain}) required to deform the separated reactants to the geometries that their respective fragments adopt in the transition state, and (b) the actual interaction energy (ΔE_{int}) that results when the deformed reactants are brought together to form the transition-state structure. The activation strain model has been fruitfully applied to understand the dramatic differences in energy profiles for S_N2@C, S_N2@Si, and S_N2@P reactions.[105,106] Similar ideas have been invoked recently in a frontier orbital analysis of the retro-Diels−Alder decomposition of o-benzyne to acetylene + diacetylene.[107]

Table 5. B3LYP/DZP++ Net Activation Barriers, Activation Strain Energies, and Transition-State Interaction Energies for S_N2 Fluoride Identity Exchange Reactions of Benzyl Derivatives[a]

	E^b (kcal mol^{-1})	ΔE_{strain} (kcal mol^{-1})	ΔE_{int} (kcal mol^{-1})
-H	−4.45	32.87	−37.32
p-CH_3	−3.40	32.58	−35.98
p-OH	−3.69	32.51	−36.20
p-OCH_3	−2.87	32.43	−35.30
p-NH_2	−1.19	32.77	−33.96
p-F	−7.22	33.14	−40.36
p-Cl	−8.85	33.01	−41.86
p-CN	−15.16	33.26	−48.42
p-NO_2	−17.54	33.95	−51.49
p-COF	−15.64	33.80	−49.44
p-CCH	−8.65	32.59	−41.24

[a] ZPVE effects are removed from the energy decomposition.

In Table 5, the net activation barriers (E^b) of the S_N2 reactions of Scheme 1 are decomposed into activation strain energies (ΔE_{strain}) and transition-state interaction energies (ΔE_{int}) on the basis of B3LYP/DZP++ computations. The ΔE_{strain} values cluster in a narrow range from 32.4 to 33.9 kcal mol^{-1}. This occurrence is indeed expected, because the geometric deformations are primarily localized on the -CH_2F moiety, whose rigidity is not substantially altered by the distant para substitutions on the aromatic ring. The near constancy of the ΔE_{strain} values means that the net activation barrier trends are mirrored in the ΔE_{int} data. Accordingly, the ranges of the E^b and ΔE_{int} values are very similar, 16.4 and 17.5 kcal mol^{-1}, respectively.

As shown in Figure 6, the transition-state interaction energy exhibits a very strong linear dependence (correlation coefficient = 0.993) on the reaction-center electrostatic potential (V_C) of the substrate. This correspondence provides an appealing physical basis for understanding V_C as a simple S_N2 reactivity index and predictor of net activation barriers. By means of the extended transition state (ETS) method,[108] the ΔE_{int} quantity can be partitioned into (a) electrostatic, (b) Pauli repulsion, and (c) charge transfer and polarization components.[102–106] The linear dependence of ΔE_{int} on V_C does not imply that the latter two components are negligible but merely that the primary driving force for transition-state interaction is electrostatic attraction, the modulation of which determines the trends in ΔE_{int}. In summary, the activation strain model provides a link for understanding how the net S_N2 barrier heights in the benzylic series of Scheme 1 are

(101) Bickelhaupt, F. M.; Ziegler, T.; Schleyer, P. v. R. *Organometallics* **1995**, *14*, 2288–2296.
(102) Bickelhaupt, F. M. *J. Comput. Chem.* **1999**, *20*, 114–128.
(103) Bickelhaupt, F. M.; Diefenbach, A. *J. Chem. Phys.* **2001**, *115*, 4030–4040.
(104) de Jong, G. T.; Bickelhaupt, F. M. *ChemPhysChem* **2007**, *8*, 1170–1181.
(105) van Bochove, M. A.; Swart, M.; Bickelhaupt, F. M. *J. Am. Chem. Soc.* **2006**, *128*, 10738–10744.
(106) Bento, A. P.; Bickelhaupt, F. M. *J. Org. Chem.* **2007**, *72*, 2201–2207.
(107) Zhang, X.; Maccarone, A. T.; Nimlos, M. R.; Kato, S.; Bierbaum, V. M.; Ellison, G. B.; Ruscic, B.; Simmonett, A. C.; Allen, W. D.; Schaefer, H. F. *J. Chem. Phys.* **2007**, *126*, 044312.
(108) (a) Ziegler, T.; Rauk, A. *Inorg. Chem.* **1979**, *18*, 1558–1565. (b) Ziegler, T.; Rauk, A. *Inorg. Chem.* **1979**, *18*, 1755–1759. (c) Ziegler, T.; Rauk, A. *Theor. Chim. Acta* **1977**, *46*, 1–10.

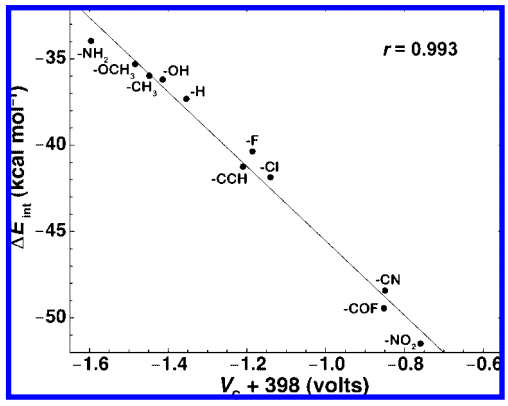

Figure 6. Relationship between transition-state interaction energy, $\Delta E_{int} = E^b - \Delta E_{strain}$, and V_C, the reaction-center electrostatic potential in the reactants of Scheme 1. Data for linear fit: *y*-intercept = −67.1(11); slope = −21.54(85); linear regression coefficient (*r*) = 0.993.

predicted by the pre-existing charge distributions in the reactants. In the $E^b = \Delta E_{strain} + \Delta E_{int}$ decomposition, the strain energy is virtually constant, while ΔE_{int} varies as the electrostatic interaction between the nucleophile and the substrate. Thus, ΔE_{int} is to a large extent proportional to the reaction-center potential V_C, regardless of whether it is evaluated at the reactant or transition-state geometry.

Summary

Bimolecular nucleophilic substitution reactions are among the most pervasively studied chemical processes, and the search for organizing principles[1] in this realm has occupied decades of research. One unifying concept is Marcus theory,[1,109] which has been established as a simple means of predicting and rationalizing the energetics and rates of S_N2 reactions. According to the Marcus expression, if the barriers for a set of S_N2 identity exchange reactions ($X^- + RX$) are known, then the barriers for all cross-reactions ($X^- + RX'$) within the group may be estimated from the corresponding reaction energies alone. In addition to myriad experiments,[110] ab initio studies[1,18,111] up to very high levels of theory have validated the Marcus approach for S_N2 reactions, with the nontransparent proviso[18] that the scheme must be applied to net barriers (E^b) rather than central barriers (E^*). To readily apply Marcus theory, simple structure−reactivity relationships are needed for predicting the intrinsic S_N2 barriers of identity exchange reactions. Toward this end, the present theoretical investigation has elucidated the structural features of benzylic compounds that make their S_N2 reactions inherently more facile than methyl analogues.

The critical effect of the aromatic ring in benzylic S_N2 systems is to raise the electrostatic potential surrounding the reaction-center carbon atom, a phenomenon unrecognized by prevailing chemical intuition. An aggrandized electrostatic propensity for nucleophilic attack results that pre-exists in the benzylic reactants and persists throughout the S_N2 process. A common explanation of the S_N2 benzylic effect posits a dynamic process whereby excess charge entering the system from the nucleophile is transferred in substantial quantities to the aromatic ring and dispersed as the reaction proceeds. Our analysis of NBO atomic charges reveals that such electron transfer is quite limited and should not be considered the primary influence on the S_N2 transition states. Strong support for an electrostatic interpretation of the benzylic effect comes from our discovery of a nearly perfect linear correlation, within the series of benzyl fluoride reactions in Scheme 1, between the net S_N2 activation barriers and the electrostatic potential (V_C) of the carbon atom at the site of nucleophilic attack. This correlation holds not only for V_C in the S_N2 transition state but also in the isolated reactant; moreover, a physical basis for the dependence is provided by the activation strain model of Bickelhaupt and co-workers.[101–106]

Ascribing an electrostatic origin to the benzylic effect has precedent in previous work on S_N2 reactions. As discussed above, experiments in the Brauman group on benzyl chloride systems can be readily interpreted by an electrostatic model,[20] although this picture is clouded in benzoyl chloride reactions.[50] With the aid of HF/6-31+G(d) computations, Streitwieser et al.[53] explained the high S_N2 reactivity of the allyl halides by electrostatic polarization of the double bond and not by conjugative effects. Another example is the $Cl^- + ClCH_2CN$ identity exchange reaction, in which the nitrile substituent greatly lowers the S_N2 barrier and dramatically accelerates the reaction rate. In 1992, this reaction was exhaustively investigated in a joint experimental/theoretical effort,[8] and substituent effects on the stability and electronic structure of S_N2 transition states were extensively discussed. As in benzylic and allylic systems, the high reactivity of chloroacetonitrile appears to be electrostatic in origin rather than a consequence of conjugative interactions in the transition state.

We have investigated the $F^- + C_6H_5CH_2F$ and $Cl^- + C_6H_5CH_2Cl$ parent reactions by ab initio focal-point computations of unprecedented rigor for S_N2 reactions of this size, incorporating electron correlation treatments with basis sets as large as valence pentuple-ζ with five d, four f, three g, and two h polarization manifolds on each heavy atom. For the benzyl fluoride system, our converged theory shows that the prereaction ion−molecule complex is bound by a remarkably large 23.4 kcal mol^{-1}, while the S_N2 barrier lies 4.6 kcal mol^{-1} *below* the isolated reactants. In the benzyl chloride case, the complexation energy is 14.8 kcal mol^{-1}, and the S_N2 barrier is 0.2 kcal mol^{-1} above the reactants. The benzylic ion−molecule complexes are significantly stabilized by an additional electrostatic interaction between the halide ion and the nearest hydrogen atom of the aromatic ring. In comparison to the (CH_3F, CH_3Cl) analogues, the ($C_6H_5CH_2F$, $C_6H_5CH_2Cl$) systems exhibit a (9.7, 3.8) kcal mol^{-1} increase in the complexation energies and a (3.8, 1.6) kcal mol^{-1} decrease in the net barrier heights. In the future, high-level focal-point results such as ours for net S_N2 barriers of selected benchmarks could be used to construct a precise functional dependence on reaction-center electrostatic potentials V_C computed by low-level density functional methods. This work would effectuate the predictive power of the simple structure−reactivity relationships established here.

Acknowledgment. B.G. acknowledges the hospitality of the Center for Computational Chemistry, University of Georgia, where most of the present computations were carried out. Professor Paul Schleyer is thanked for comments on the manuscript. The research in Georgia was supported by the National Science Foundation, Grant CHE-0749868; the research in Sofia was supported by the National Science Fund (Bulgaria), Grant VU-980/05. Massively parallel computations were performed at the Pittsburgh Supercomputing Center and the National Center for Supercomputing Applications

(109) Marcus, R. A. *Annu. Rev. Phys. Chem.* **1964**, *15*, 155.
(110) Wladkowski, B. D.; Brauman, J. I. *J. Phys. Chem.* **1993**, *97*, 13158–13164.
(111) Wolfe, S.; Mitchell, D. J.; Schlegel, H. B. *J. Am. Chem. Soc.* **1981**, *103*, 7694–7696.

at the University of Illinois, Urbana−Champaign, through TeraGrid Grant TG-CHE070039N.

Supporting Information Available: Plots of B3LYP/DZP++ computed net barriers (E^b) versus focal-point benchmarks, and charge transferred in the benzylic transition states to the aromatic ring; focal-point analyses of the $C_6H_5CH_2F/F^-$ and $C_6H_5CH_2Cl/Cl^-$ complexation energies; Cartesian coordinates of all optimized geometric structures; and complete refs 89 and 90. This material is available free of charge via the Internet at http://pubs.acs.org.

JA802246Y